Na$_4$SnS$_4$ and Na$_4$SnSe$_4$ exhibiting multifunctional physicochemical performances as potential infrared nonlinear optical crystals and sodium ion conductors

Lihua Gao, Gang Bian, Ya Yang, Bingbing Zhang, Xiaowen Wu,* Kui Wu*

College of Chemistry and Environmental Science, Hebei University, Baoding 071002, China

To whom correspondence should be addressed :

E-mails: wukui@hbu.edu.cn (Kui Wu)

CONTENTS

1. Synthesis of Title Compounds

Initial reagents with high purity ($\geq$ 99.9%) including Na_2S, Na_2Se, SnS_2 and $SnSe_2$, were directly purchased from the Beijing Hawk Science & Technology Co., Ltd. Whole preparation process was completed in an Ar-filled glovebox because of the instability for Na_2S and Na_2Se in the air. Their reaction processes were achieved in the vacuum-sealed silica tubes by the high-temperature muffle furnace. Title compounds were successfully synthesized under the sinter temperature at 500 ^{o}C for several days and then cool to room temperature with the rate at 5 ^{o}C/h. Pale yellow crystals with high yield (>95 %) in Na_4SnS_4 were achieved. Deep-yellow crystals of Na_4SnSe_4 were found in silica tubes. Among them, Na_4SnSe_4 is hydroscopic and dissolve in water and Na_4SnS_4 is relatively stable in the air.

2. Structural Refinement and Crystal Data

Selected high-quality crystals were used for data collections on a Bruker SMART APEX II 4K CCD diffractometer using Mo Kα radiation (λ = 0.71073 Å) at 296 K. The crystal structures were solved by direct method and refined using the SHELXTL program package. Multi-scan method was used for absorption correction. Rational anisotropic thermal parameters for all atoms were obtained by the anisotropic refinement and extinction correction. PLATON was also used to check the final structures and no other symmetries were found. Detail refinement parameters and data were shown in Table S1.

3. Property Characterization

3.1 Powder X-ray Diffraction

Powder X-ray diffraction (XRD) patterns of title compounds were collected on a Bruker D2 X-ray diffractometer with Cu Kα radiation (λ = 1.5418 Å) at room temperature. The 2θ range was 10-70 ° with a step size of 0.02 ° and a fixed counting time of 1s/step. In order to avoid the moisture absorption of micro-crystals, we have to test their powder XRD in the custom-made vacuum-sealed apparatus and the sample loading process was completed in the Ar-atmosphere glovebox.

3.2 UV−Vis−Near-IR (NIR) Diffuse-Reflectance Spectra

Diffuse-reflectance spectra were measured by a Shimadzu SolidSpec-3700DUV spectrophotometer in the wavelength range of 200−1100 nm at room temperature. The sample-loading process was completed in the Ar-atmosphere glovebox and we used the highly transparent quartz plate on sealing the sample to keep the air out.

3.3 Raman spectra

Hand-picked crystals were first put on an object slide, and then a LABRAM HR Evolution spectrometer equipped with a CCD detector by a 532 nm laser was used to record the Raman spectra. The integration time was set to be 5 s. In view of the extremely short test time (< 30 s) in whole testing process, this test does not need the vacuum protection.

3.4 Second-harmonic Generation Measurement

Through the Kurtz and Perry method, powder SHG responses of title compounds were investigated by a Q-switch laser (2.09 μm, 3 Hz, 50 ns) with different particle sizes, including 38−55, 55−88, 88−105, 105−150, 150−200, and 200−250 μm. The $AgGaS_2$ crystal was ground and sieved into the same size range as the reference. The sample-loading process in sample-box was completed in the Ar-atmosphere glovebox and then the sample box was further sealed use the sealant.

3.5 LDT Measurement

The LDTs of title compounds were evaluated on powder sample (150−200 μm) with a pulsed YAG laser. Similar size of $AgGaS_2$ is chosen as the reference. To adjust different laser beams, an optical concave lens is added into the laser path. The damage spot is measured by the scale of optical microscope. This vacuum protection process is similar to that of SHG measurement.

3.6 Conductivity Measurements

The electrochemical impedance spectra (EIS) of title compounds have measured by an electrochemical workstation (Biologic, VSP) and the frequency ranged from 1MHz to 1Hz. All the tabletting and drying processes are completed in the glovebox. Powder sample of three compounds were pelleted with a thickness of approximate 1mm and a diameter of 13mm under 20 ton of pressure. Then taking these pellets on one heating

plate about 3-5 h after covering silver paste in the glovebox. The pellets were plated into one special sealed box with electrode on both ends. The temperature-dependent AC impedance spectra for title compounds were studied at different temperature from 20 to 70 ℃ with an increment of 10 ℃. The ionic conductivity was obtained through the equation $\sigma = L/S \cdot R$, where L is pelleted thickness, S is the area, and the total resistance R is equal to real impedance when imaginary impedance approaches zero ($Z'' \approx 0$). After this test, the pellets show no sign of moisture absorption.

3.7 Computational Description

Utilized the plane-wave pseudopotential method implemented in the CASTEP, the electronic structures of title compounds were performed on DFT. All of them were optimized by The Perdew-Burke-Ernzerhof (PBE) exchange-correlation of Generalized Gradient Approximation (GGA). A Kleinman-Bylander representation of the ultrasoft pseudopotential is automatically introduced and the valance electrons of the related atoms were: Na $2s^2 3s^1$, Sn $5s^2 5p^2$, S $3s^2 3p^4$ and Se $4s^2 4p^4$, respectively. Also, kinetic energy cut-offs were set to be 600.0 eV with a density of fewer than 0.05 $Å^{-1}$ in the Brillouin zone (BZ) was adopted. As important parameters for NLO crystals, SHG coefficient and birefringence were also calculated with suitable scissors operators.

4. Figures and Tables

Table S1. Crystal data and structure refinement for title compounds.

Table S2. Coordination environments of Na and Sn atoms in the Na-Sn-Se system.

Table S3. Comparison on LDTs between title compounds and $AgGaS_2$.

Table S4. Ionic conductivities in title compounds at different temperatures.
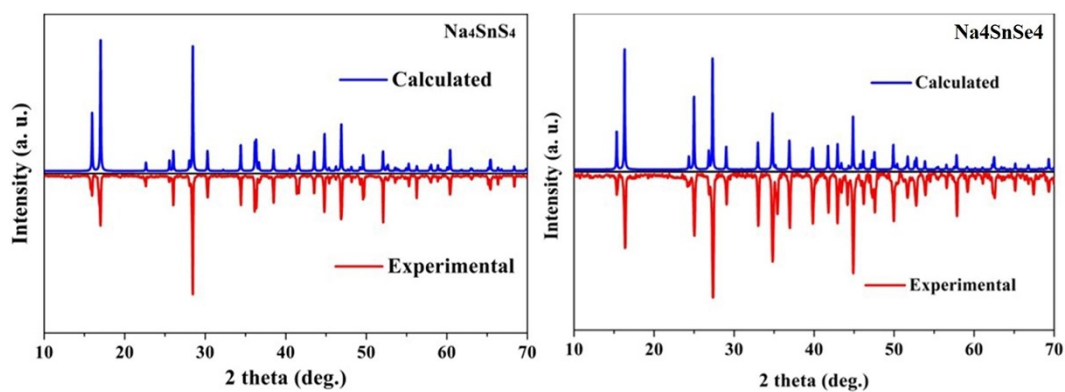
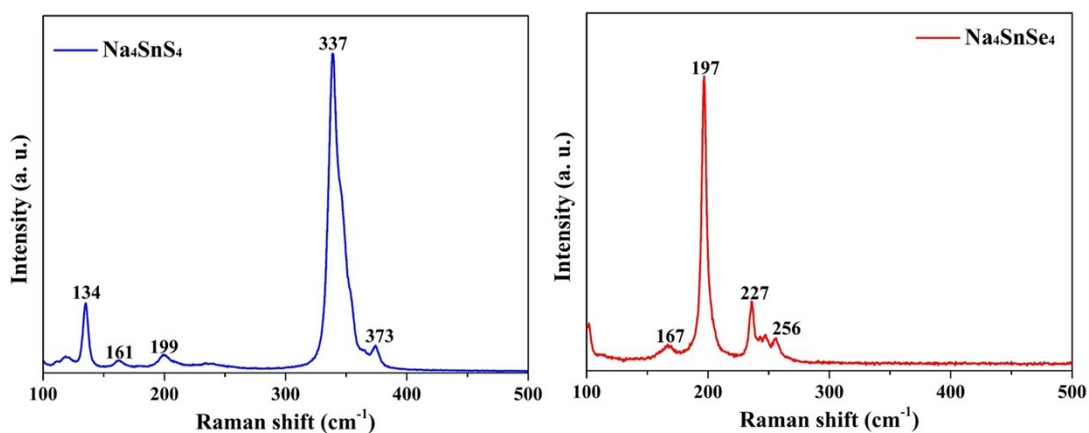**Figure S1**. Powder XRD patterns of title compounds.

Figure S2. Raman spectra of title compounds.

Figure S3. Calculated electronic structures of title compounds.

Figure S4. Powder SHG response *versus* particle size among title compounds and $AgGaS_2$ (as a reference).

Figure S5. SHG density at the occupied and unoccupied states in Na_4SnSe_4.

Table S1. Crystal data and structure refinement for title compounds.

Empirical formula	Na_4SnS_4	Na_4SnSe_4
formula weight	338.89	526.49
crystal system	Tetragonal	Tetragonal
space group	$P\bar{4}2_1c$	$P\bar{4}2_1c$
cell parameter a (Å)	7.8419(6)	8.1674(7)
cell parameter c (Å)	6.9522(9)	7.2665(13)
Z, V (Å^3)	2, 427.53(9)	2, 484.72(12)
D_c (g/cm^3)	2.633	3.607
μ (mm^{-1})	4.071	17.748
goodness-of-fit on F^2	1.051	0.933
R_1, wR_2 (I > 2σ(I))[a]	0.0117,0.0214	0.0202,0.0414
R_1, wR_2 (all data) [a]	0.0127,0.0216	0.0225,0.0419
absolute structure parameter	-0.01(3)	0.034(18)
largest diff. peak and hole (e·Å^{-3})	0.194,–0.216	0.529,–0.392

[a]$R_1 = F_o - F_c / F_o$ and $wR_2 = [w (F_o^2 - F_c^2)^2 / wF_o^4]^{1/2}$ for $F_o^2 > 2\sigma (F_o^2)$

Table S2. Coordination environments of Na and Sn atoms in the Na-Sn-Se system.

compounds	Space group	NaSe$_n$	SnSe$_n$ and link modes
$Na_6Sn_2Se_7$	C2/c	$n = 4, 6$	4, $[Sn_2Se_7]^{6-}$
$Na_2Sn_2Se_5$	Pbca	$n = 6, 7$	4, 2D layer
α-Na_2SnSe_3	$P2_1/c$	$n = 5, 6$	4, $(SnSe_3)_n$ chain
β-Na_2SnSe_3	Pnma	$n = 5, 6$	4, $(SnSe_3)_n$ chain
Na_4SnSe_4	$P\bar{4}2_1c$	$n = 5$	4, $[SnSe_4]^{4-}$

Table S3. Comparison on LDTs between title compounds and $AgGaS_2$.

compounds	damage energy (mJ)	spot diameter (mm)	LDT (MW/cm^2)	LDT (× AGS)*
$AgGaS_2$	0.58	0.5	29.6	1
Na_4SnS_4	5.24	0.5	267	9.0
Na_4SnSe_4	2.05	0.5	104	3.5

*AGS = $AgGaS_2$

Table S4. Ionic conductivities in title compounds at different temperatures.

σ_T (S/cm) Compounds	Na_4SnSe_4	Na_4SnS_4
20 ℃	1.132×10^{-8}	1.423×10^{-8}
30 ℃	2.188×10^{-8}	2.176×10^{-8}
40 ℃	3.431×10^{-8}	4.530×10^{-8}
50 ℃	4.798×10^{-8}	8.710×10^{-8}
60 ℃	6.291×10^{-7}	1.623×10^{-7}
70 ℃	8.788×10^{-7}	5.631×10^{-7}

Figure S1. Powder XRD patterns of title compounds.

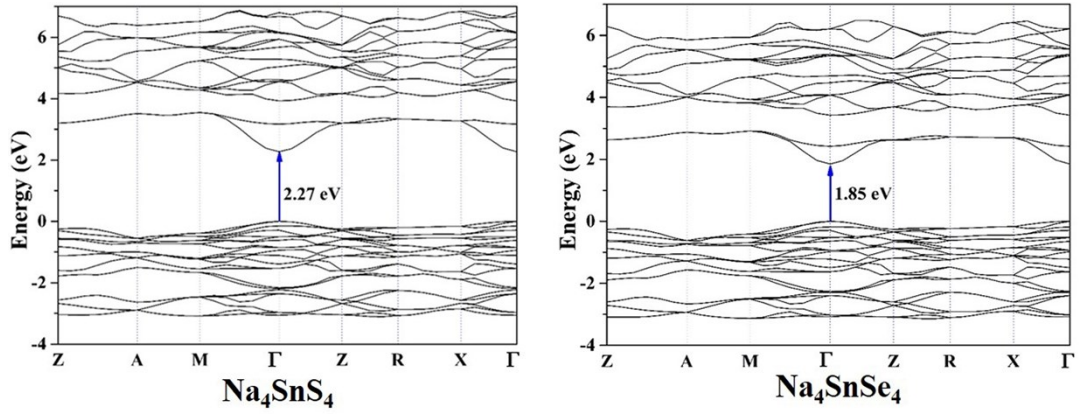**Figure S2**. Raman spectra of title compounds.

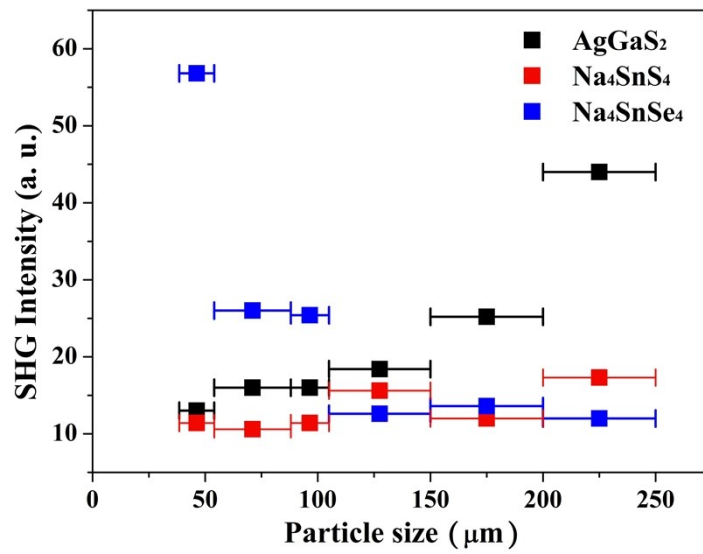**Figure S3**. Calculated electronic structures of title compounds.

Figure S4. Powder SHG response *versus* particle size among title compounds and AgGaS$_2$ (as a reference).
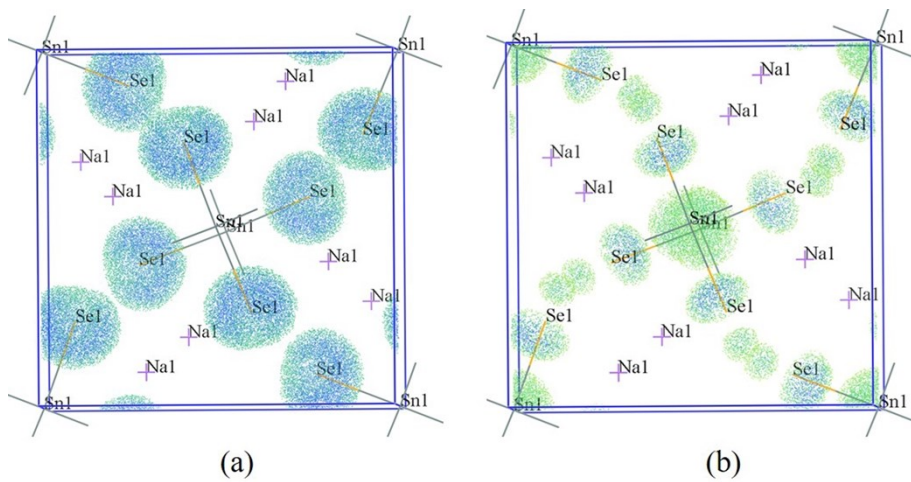

Figure S5. SHG density at the occupied (a) and unoccupied (b) states in Na$_4$SnSe$_4$.